Biochemical Pharmacology, Vol. 28, pp. 2891–2908

0006-2952/79/1001-2891 $02.00/0

PHARMACO-ENZYME KINETIC SIMULATIONS OF EXPERIMENTAL INTERACTIONS AMONG MULTIPLE ANTINEOPLASTIC DRUGS

CLAUDIO A. NICOLINI, ANDREW BELMONT, MASSIMO GRATTAROLA, COLLEEN MOORE * and ELLIOTT MILGRAM

Division of Biophysics, Temple University Graduate School, Philadelphia, PA 19140, U.S.A.

(*Received* 14 *October* 1978; *accepted* 12 *January* 1979)

Abstract—Several models of DNA synthesis based on enzyme kinetics are examined, the most inclusive of them referring to *in vivo* simulations. They are open systems based on Michaelis–Menten kinetics for enzymes of deoxynucleotide and DNA synthesis, and incorporate complex biochemical feedback controls as well as intracellular nucleotide and enzyme concentrations. Both steady state and transient situations have been studied. The responses of such systems to single and multiple administration of drugs under steady state conditions, and to single and time-sequenced multiple drug administration under transient conditions are described and compared to available experimental results. In the process, a quantitative drug index is defined to describe the interaction of two or more drugs at steady state conditions. Our simulations demonstrate that it may be possible to reverse the type, as well as the intensity, of the interaction between two drugs by increasing the concentration of a third drug, and that transient deviations from steady state pool sizes may have profound influence on drug action in a manner which cannot be predicted by steady state results. In particular, a change in the order of two drugs given sequentially may give rise to significant differences in total DNA synthesis. Finally, our results indicate a strong sensitivity of the model to small structural or quantitative changes. This suggests that variations in enzyme activities observed among different cell lines will give rise to differential drug responses which may be simulated properly only by a realistic model, utilizing real values for all constants and including all known pathways. Preliminary results with such a model are described.

In the past several years, knowledge concerning the biological synthesis of nucleic acids has grown steadily [1]. The picture emerging is that of a complex and still incompletely understood system of reactions tightly regulated through a network of feedback and activation controls. For such a system, standard explanations derived from concepts of sequential, concurrent, and complementary inhibition [2] are simply not applicable in understanding the overall action of inhibitors of nucleic acid synthesis [3].

As a first step toward the development of a theoretical framework for the understanding of exactly such results, Werkheiser *et al.* [3] devised a simple mathematical model which simulated the effect of combinations of inhibitors of DNA synthesis on cell growth *in vitro*. Recently, we have extended such work by introducing several new enzyme kinetic models, all based on open systems regulated by a network of feedback controls, which, together, represent a logical progression toward our ultimate goal of analyzing the effects of combinations of DNA antimetabolites *in vivo*.

In an earlier publication [4], we described the computer algorithms developed to solve the nonlinear algebraic and differential equations encountered without the arbitrary simplifications previously utilized [3, 5, 6]. It is the purpose of this paper to describe the results obtained by increasing the complexity of our models to include all known DNA metabolic pathways and new pharmaco-enzyme interaction data available from various laboratories, and to discuss how these results have guided us in our design of a realistic *in vivo* model. In addition, we will document new quantitative techniques and concepts acquired in our studies, including multiple drug interactions and time sequence drug administration, which we believe may be important tools for any pharmaco-enzyme kinetic study and for planning an effective combination drug cancer chemotherapy.

DESCRIPTION OF THE MODELS

We have created several alternative models under the common assumption of an open system in which the concentrations of nucleotide diphosphates are held constant (a valid approximation, given that the rate of DNA production is small relative to the other diphosphate reaction rates) and in which the DNA polymer product serves as an absolute sink. All enzymes including DNA polymerase are assumed to operate according to simple Michaelis–Menten rate equations and, where included, inhibitory and activating feedback controls arising from various intermediate concentrations are approximated by a simple competitive type interaction.

In the first three models (DNAMET I, II, and III), the concentrations of all substrates and inhibitors are represented in terms of specific concentrations, i.e. molar concentration divided by Michaelis constant (K_m) or by an inhibition constant (K_i) [7]. In addition, in these models all constants are set equal to 0 or 1 for the mathematical simulation (except where indicated otherwise).

The modes of action of each of the drugs considered were based on the current consensus, as expressed in the

* Department of Biochemistry, M. D. Anderson, Hospital and Tumor Institute, Houston, TX.

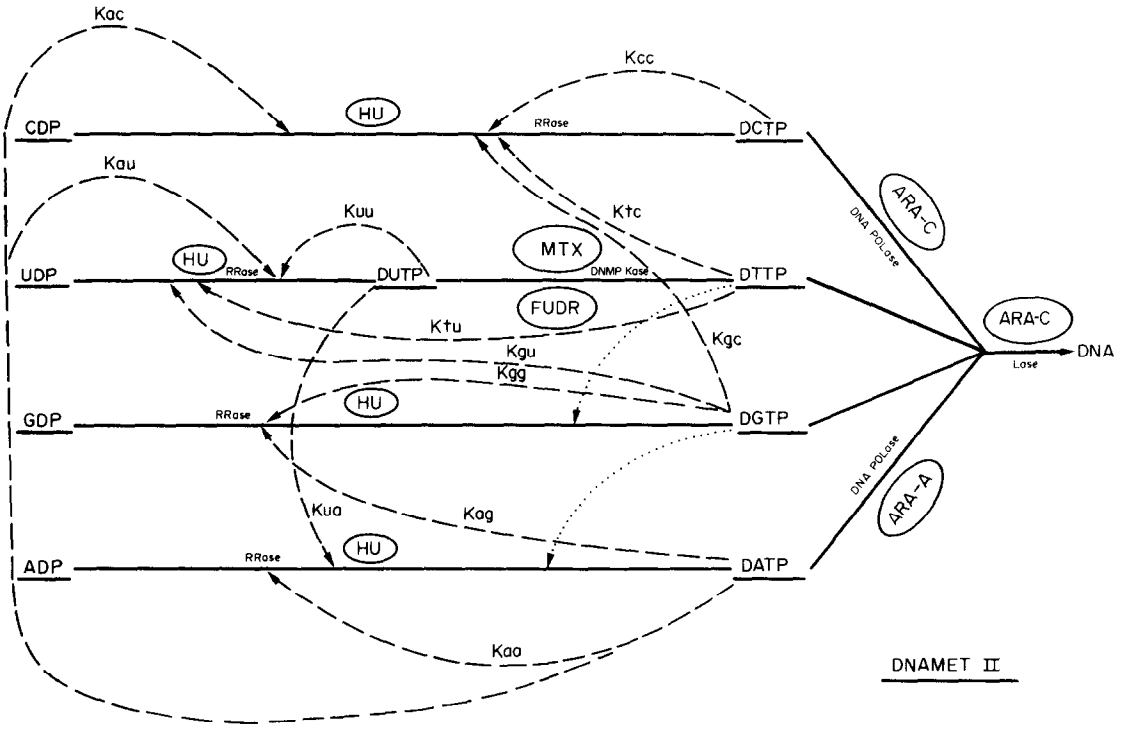
Kac
Kcc
CDP
HU
RRase
DCTP
Kau
Kuu
Ktc
ARA-C
DNA POLase
MTX
HU
RRase
UDP
DUTP
DNMP Kase
DTTP
FUDR
Ktu
Kgu
Kgc
Kgg
ARA-C
Lase
DNA
HU
GDP
RRase
DGTP
Kua
Kag
DNA POLase
ARA-A
HU
ADP
RRase
DATP
Kaa
DNAMET II

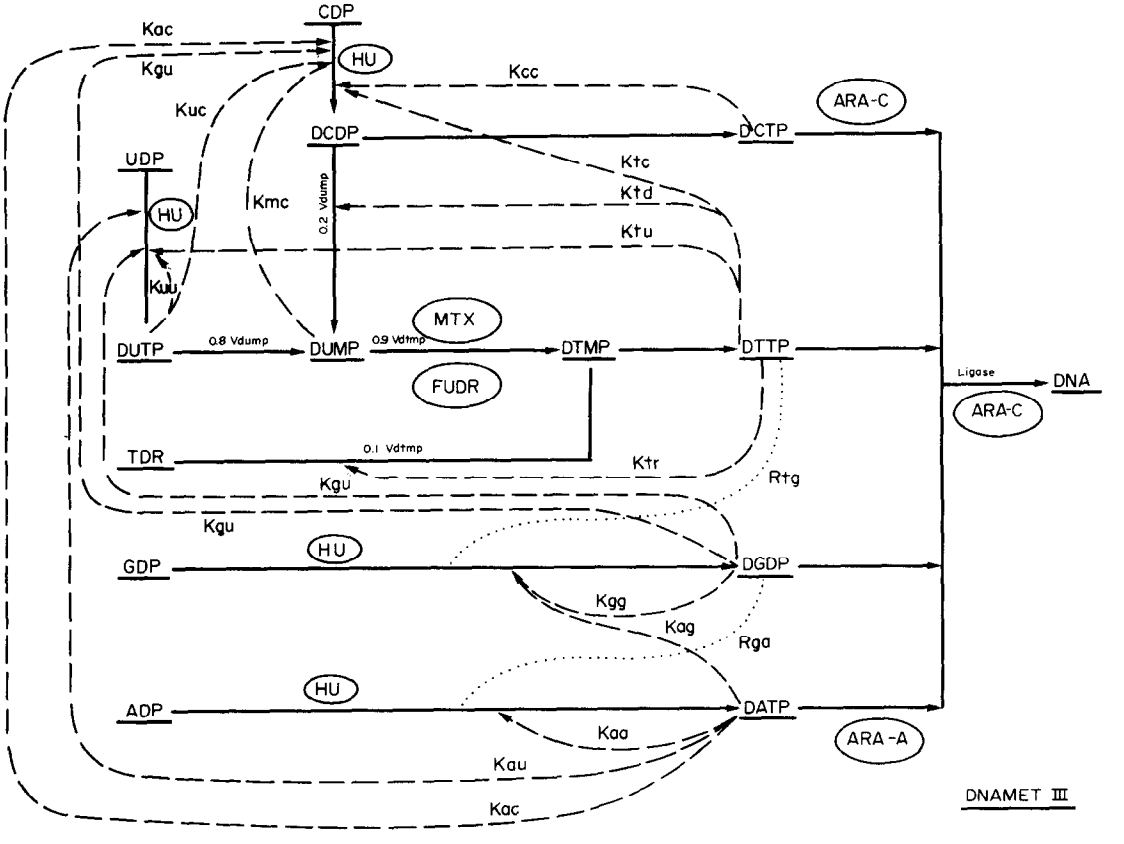
CDP
Kac
Kgu
HU
Kcc
Kuc
ARA-C
DCDP
DCTP
UDP
Ktc
Ktd
Kmc
0.2 Vdump
HU
Ktu
Kuu
MTX
DUTP
0.8 Vdump
DUMP
0.9 Vdtmp
DTMP
DTTP
Ligase
DNA
FUDR
ARA-C
TDR
0.1 Vdtmp
Ktr
Rtg
Kgu
Kgu
HU
GDP
DGDP
Kgg
Kag
Rga
HU
ADP
DATP
Kaa
ARA-A
Kau
Kac
DNAMET III

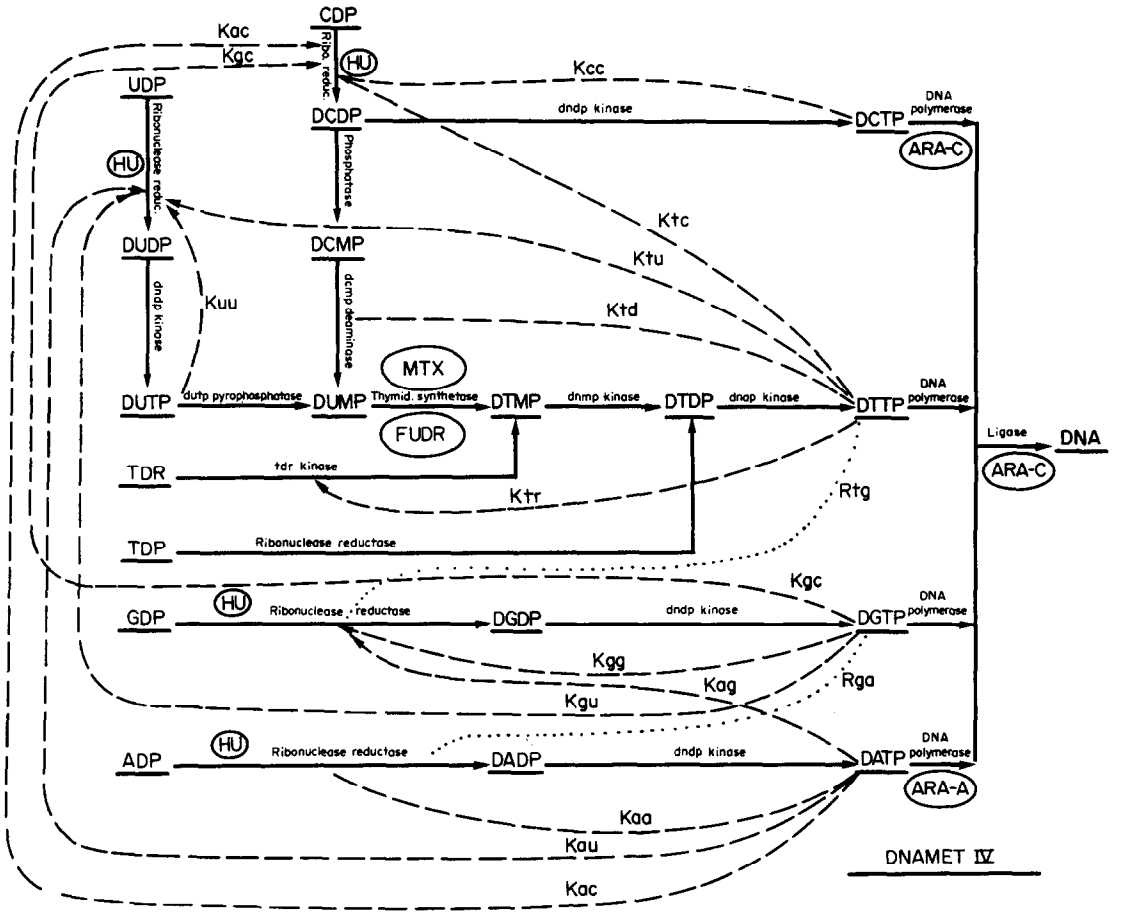

Fig. 1. Schematics of the models DNAMET II, III and IV. Solid lines show interconversions (———). Dashed lines refer to feedback inhibition pathways (---). Dotted lines refer to feedback activating pathways (...).

recent literature [1, 8]. Unfortunately, this consensus was often difficult to define as considerable controversy and uncertainty still exist over the molecular mechanisms involved in the actions of these drugs. ARA-C (1-β-D-arabinofuranosylcytosine), a nucleotide analogue with a configuration similar to that of cytidine and deoxycytidine, is generally considered to be a competitive inhibitor [9] of DNA synthesis through the action of its 5′-triphosphate, ARA-CTP, on the polymerization of deoxyribonucleotides [10]. It has also been shown to interfere, perhaps in a complex fashion, with the reduction of cytidine diphosphate [9] and to have an effect on DNA elongation [11]. Hydroxyurea (HU) has been shown to be a potent inhibitor of DNA synthesis by acting as a noncompetitive inhibitor with all ribonucleotide reductases [12]. However, experiments designed to reverse the inhibition by the addition of deoxyribonucleotides have had limited success [12], and this casts doubt on a single site of action [13, 14]. Fluorodeoxyuridine (FUDR) seems to be a competitive inhibitor of thymidylate synthetase [15], but through complex and obscure feedback mechanisms other sites of action in the DNA metabolic pathway are affected, while methotrexate (MTX) can be approximated as a noncompetitive inhibitor of thymidylate synthetase [3]. ARA-A (9-β-D-arabinofuranosyladenine), which inhibits DNA polymerase in competition with the adenine pool, also may have more than one site of action in the DNA metabolic pathway.

In model DNAMET I, Werkheiser's original model, only those enzymes directly affected by the drugs considered were included [3]. Additional enzymes were added in the later models (II, III and IV) in order to include additional feedback controls, to include more completely the effects of HU and ARA-C, and to include salvage pathways which were viewed as important in simulating *in vivo* conditions. Detailed descriptions of each model are provided below.

DNAMET I: This is identical to Werkheiser's original model [3]. For a schematic of the model and a listing of the algebraic and differential equations the reader is referred to the original papers [3, 4].

DNAMET II: Several modifications are present in model II, represented in Fig. 1. One is the inclusion of the guanine pathway GDP→DGTP→DNA. This provides a more complete simulation of the action of HU and an increase in the feedback control of the overall system through the presence of inhibitory pathways arising from DGTP. It also provides the possibility of including in the simulation two activating feedback

Michaelis–Menten equations from model DNAMET II

$$v_{\mathrm{DCTP}} = \frac{V_{\max}^{\mathrm{DCTP}}}{\{[1 + 1/\mathrm{CDP}(1 + \mathrm{DCTP}\cdot K_{cc} + \mathrm{DTTP}\cdot K_{tc} + \mathrm{DGTP}\cdot K_{gc} + \mathrm{DATP}\cdot K_{ac})](1 + \mathrm{HU})\}}$$

$$v_{\mathrm{DUTP}} = \frac{V_{\max}^{\mathrm{DUTP}}}{\{[1 + 1/\mathrm{UDP}(1 + \mathrm{DUTP}\cdot K_{uu} + \mathrm{DTTP}\cdot K_{tu} + \mathrm{DGTP}\cdot K_{gu} + \mathrm{DATP}\cdot K_{au})](1 + \mathrm{HU})\}}$$

$$v_{\mathrm{DTTP}} = \frac{V_{\max}^{\mathrm{DTTP}}}{\{[1 + 1/\mathrm{DUTP}(1 + \mathrm{FUDR})](1 + \mathrm{MTX})\}}$$

$$v_{\mathrm{DGTP}} = \frac{V_{\max}^{\mathrm{DGTP}}}{\{[1 + 1/\mathrm{GDP}\,1 + \mathrm{DGTP}\cdot K_{gg} + \mathrm{DATP}\cdot K_{ag}/1 + \mathrm{DTTP}\cdot R_{tg})](1 + \mathrm{HU})\}}$$

$$v_{\mathrm{DATP}} = \frac{V_{\max}^{\mathrm{DATP}}}{\{[1 + 1/\mathrm{ADP}(1 + \mathrm{DUTP}\cdot K_{ua} + \mathrm{DATP}\cdot K_{aa}/1 + \mathrm{DGTP}\cdot R_{ga})](1 + \mathrm{HU})\}}$$

$$v_{\mathrm{DNA}} = \frac{5}{\{1.5/V_{pc}[1 + 1/\mathrm{DCTP}(1 + \mathrm{ARA\text{-}C})] + 1/V_{dt}[1 + 1/\mathrm{DTTP}] + 1.5/V_{dg}[1 + 1/\mathrm{DGTP}] + 1/V_{da}[1 + 1/\mathrm{DATP}](1 + \mathrm{ARA\text{-}A})\}(1 + \mathrm{ARA\text{-}C})}$$

Differential equations from model DNAMET II

$$\frac{\mathrm{d}}{\mathrm{d}t}(\mathrm{DCTP}) = v_{\mathrm{DCTP}} - v_{\mathrm{DNA}}$$

$$\frac{\mathrm{d}}{\mathrm{d}t}(\mathrm{DUTP}) = v_{\mathrm{DUTP}} - v_{\mathrm{DTTP}}$$

$$\frac{\mathrm{d}}{\mathrm{d}t}(\mathrm{DTTP}) = v_{\mathrm{DTTP}} - v_{\mathrm{DNA}}$$

$$\frac{\mathrm{d}}{\mathrm{d}t}(\mathrm{DGTP}) = v_{\mathrm{DGTP}} - v_{\mathrm{DNA}}$$

$$\frac{\mathrm{d}}{\mathrm{d}t}(\mathrm{DATP}) = v_{\mathrm{DATP}} - v_{\mathrm{DNA}}$$

Michaelis–Menten equations from model DNAMET IV

$$v_{\mathrm{DUDP}} = \frac{V_{\max}^{\mathrm{DUDP}}}{[1 + K_m^{\mathrm{UDP}}/\mathrm{UDP}(1 + \mathrm{DTTP}/K_{tu} + \mathrm{DGTP}/K_{gu} + \mathrm{DATP}/K_{au} + \mathrm{DUTP}/K_{uu})](1 + \mathrm{HU}/K_i^{\mathrm{HU}})}$$

$$v_{\mathrm{DUTP}} = \frac{V_{\max}^{\mathrm{DUTP}}}{1 + K_m^{\mathrm{DUDP}}/\mathrm{DUDP}}$$

$$v_{\mathrm{DCDP}} = \frac{V_{\max}^{\mathrm{DCDP}}}{[1 + K_m^{\mathrm{CDP}}/\mathrm{CDP}(1 + \mathrm{DTTP}/K_{tc} + \mathrm{DGTP}/K_{gc} + \mathrm{DATP}/K_{ac})](1 + \mathrm{HU}/K_i^{\mathrm{HU}})}$$

$$v_{\mathrm{DCTP}} = \frac{V_{\max}^{\mathrm{DCTP}}}{[1 + K_m^{\mathrm{DCDP}}/\mathrm{DCDP}(1 + \mathrm{DCTP}/K_{cc})]}$$

$$v_{\mathrm{DCMP}} = \frac{V_{\max}^{\mathrm{DCMP}}}{1 + K_m^{\mathrm{DCDP}}/\mathrm{DCDP}}$$

$$v_{\mathrm{T1}} = \frac{V_{\max}^{\mathrm{T1}}}{1 + K_m^{\mathrm{DCMP}}/\mathrm{DCMP}(1 + \mathrm{DTTP}/K_{td})}$$

$$v_{\mathrm{T2}} = \frac{V_{\max}^{\mathrm{T2}}}{1 + K_{\max}^{\mathrm{DUTP}}/\mathrm{DUTP}}$$

$$v_{\mathrm{DUMP}} = v_{\mathrm{T1}} + v_{\mathrm{T2}}$$

$$v_{\mathrm{T3}} = \frac{V_{\max}^{\mathrm{T3}}}{[1 + K_m^{\mathrm{DUMP}}/\mathrm{DUMP}(1 + \mathrm{FUDR}/K_i^{\mathrm{FUDR}})](1 + \mathrm{MTX}/K_i^{\mathrm{MTX}})}$$

$$v_{\mathrm{T4}} = \frac{V_{\max}^{\mathrm{T4}}}{1 + K_m^{\mathrm{TDR}}/\mathrm{TDR}(1 + \mathrm{DTTP}/K_{tr})}$$

$$v_{DTMP} = v_{T3} + v_{T4}$$

$$v_{T5} = \frac{V_{max}^{T5}}{1 + K_m^{DTMP}/DTMP}$$

$$v_{T6} = \frac{V_{max}^{T6}}{1 + K_m^{TDP}/TDP(1 + HU/K_i^{HU})}$$

$$v_{DTDP} = v_{T5} + v_{T6}$$

$$v_{DTTP} = \frac{V_{max}^{DTTP}}{1 + K_m^{DTDP}/DTDP}$$

$$v_{DGDP} = \frac{V_{max}^{DGDP}}{\left[1 + K_m^{GDP}/GDP\left(\frac{1 + DGTP/K_{gg} + DATP/K_{ag}}{1 + DTTP/R_{tg}}\right)\right](1 + HU/K_i^{HU})}$$

$$v_{DGTP} = \frac{K_{max}^{DGTP}}{1 + K_m^{DGDP}/DGDP}$$

$$v_{DADP} = \frac{V_{max}^{DADP}}{\left[1 + K_m^{ADP}/ADP\left(\frac{1 + DATP/K_{aa}}{DGTP/R_{ga}}\right)\right](1 + HU/K_i^{HU})}$$

$$v_{DATP} = \frac{V_{max}^{DATP}}{1 + K_m^{DADP}/DADP}$$

$$v_{DNA} = \frac{5}{\{[1.5/V_{max}^{CD}(1 + K_m^{DCTP}/DCTP)(1 + ARA\text{-}C/K_i^{ARA\text{-}C}) + 1/V_{max}^{TD}(1 + K_m^{DTTP}/DTTP) + 1/V_{max}^{GD}(1 + K_m^{DGTP}/DATP)(1 + 1/V_{max}^{AD})(1 + K_m^{DATP}/DATP)(1 + ARA\text{-}A/K_i^{ARA\text{-}A})](1 + ARA\text{-}C/K_i^{ARA\text{-}C})\}}$$

Fig. 2. Michaelis-Menten equations for model II and model IV (see Fig. 1 for the schematics of the models). The differential equations for model II are also given.

pathways, namely DTTP activating the DGP→DGTP pathway and DGTP activating the ADP→DATP pathway. Another more general change is the inclusion of additional inhibitory feedback pathways interlinking the various nucleotide synthesis pathways.

Perhaps the most important difference is the additional reaction step catalyzed by the ligase enzyme. This is significant in permitting the consideration of the action of ARA-C on the ligase step. (An interesting speculation is that this effect of ARA-C on the ligase may relate to the fact that ARA-C becomes [11] cytotoxic just above levels of DNA inhibition produced by other drugs at concentrations well below their own threshold for cytotoxicity.) Because the literature was vague about the specific type of interaction involved in this pathway, both competitive and noncompetitive actions were initially simulated. Due to the nature of the isobols generated in each case (described later in this paper) relative to the experimental isobols of Grindey and Nichol [5], it was decided to treat ARA-C as a noncompetitive inhibitor of ligase (confirmed later by biochemical assays).

Finally, a change was made in the last step of the metabolic pathway described by Eqn. 6 for model II in Fig. 2. This change is readily understandable after one briefly reviews the rationale for the corresponding equation of model I.That equation was derived under the assumption that the enzyme obeys simple Michaelis–Menten kinetics with respect to the corresponding deoxynucleotide triphosphates, and that the product can be considered a random trimer of DATP, DCTP and DTTP. Therefore, the time for synthesis of the trimer was taken as the sum of the times required to assemble each precursor.

There, the statistical factor of 3 takes into account that the incorporation of each component represents only one third of the total reaction. In model II there are only two differences to be recognized. First, there are now four precursors, and second, we are incorporating the empirical ratio between the various nucleotides in the final product by weighting the DCTP and DGTP terms by a factor of 150 per cent. Thus, the statistical factor necessary is now 5.

This model is more closely similar to a later model developed by the Werkheiser group [6], although it differs in many of the details and in the presence of a ligase step.

As a preliminary test for the effect of the introduction of real values on predictions of the model, we also studied a version of model II with all the constants as close as possible to the experimental values. For the most part, we used the same constants used in model IV described below. In several cases, however, where several steps of model IV were collapsed into a single step in model II, we chose the maximal velocity of the slowest step to represent the maximal velocity of the analogous single step in model II.

DNAMET III: Additional modifications and addi-

tions were made to model II, yielding model III. (See Fig. 1 for the schematic diagram of model DNAMET III.) These changes are as follows:

(1) Inclusion of the branching pathway

DCDP → DCTP
↓
DUMP → DTMP

(2) TDR → DTMP (salvage pathway)
(3) The additional feedback inhibition pathways.

A problem arose in regard to handling the branching pathways. An example is the formation of DUMP. This intermediate compound is produced from DUTP → DUMP, and from DCDP → DUMP. We made the assumption that the ratio of the maximal velocity of DUMP formation from DCDP to the maximal velocity of DUMP formation from DUTP is 1:4. This assumption, in conjunction with the fact that, at infinite concentrations of the substrates DCDP and DUTP, the velocity of formation of DUMP (v_{DUMP}) must equal the maximal velocity (V_{max}^{DUMP}), enables us to write the equation describing the velocity of formation of DUMP as found in Fig. 2. The same problem arose with DTMP because, like DUMP, it was formed from two different pathways:

DUMP → DTMP

and

TDR → DTMP

Here we assumed that the ratio of the maximal velocity of DTMP formation from DUMP to the maximal velocity of DTMP formation from TDR is 9:1. Again, at infinite concentrations of the substrates DUMP and TDR, the velocity of formation of DTMP must equal V_{max}^{DTMP}, so we can write the equation describing the velocity of DTMP formation as found in Fig. 2.

DNAMET IV: The design of model IV was guided by preliminary investigations with regard to attaining a steady state of the transitional model DNAMET III, also shown in Fig. 1. Model IV represents a large step forward in progress toward our ultimate goal. Realistic values for all constants, maximal velocities, inhibition and activation constants, Michaelis constants, and even starting concentrations, have been employed. These values are the result of numerous biochemical assays, conducted in various cell lines, and for the most part are extracted (under the assumption of homogenous distribution of chemicals over cell volume) from the results of recent experiments, both published and unpublished. In many cases the given value was selected from several figures, obtained from different cell lines or by varying experimental techniques (see Table 2). This range of values, where included, was very important to us in indicating the degree of freedom we had in adjusting these constants during the course of our investigations. In Table 1 we have compiled those values initially suggested by the biochemical assays and have indicated which were purely estimates made without recourse to any direct supporting data, which were fixed roughly by a single experimental value, and which were based within a certain range by several experimental values. In Table 1 we have also presented those values currently in use.

Besides the switch to "real" constants from arbitrary and uniform constants, other major changes in model IV are the inclusion of both salvage pathways TDP → DTDP and TDR → DTMP, and the inclusion of all deoxyribonucleotide diphosphate intermediates.

With constant feedback between the mathematical simulation and the empirical biochemical findings, this model, now the focus of our attention, is in a state of constant flux. However, despite the difficulty such an interaction creates, we feel this approach is essential for the acquisition of meaningful results, as it presents results in terms of real concentrations and real time. This difference from the previous models is crucial for the development of an optimal chemotherapy strategy based on enzyme kinetics and for allowing planned studies of time sequence simulations of drug interaction. Figure 2 shows the Michaelis–Menten equations for model DNAMET IV.

Mathematical methods

It is only by benefit of sophisticated mathematical treatment that we have been able to demonstrate our flexibility in model building. All work is performed through numerical algorithms run either on the CDC 3600 or PDP11 computer. Time evolution studies have been carried out for models I and II using Hamming's modified predictor–corrector method [16]. By the application of this method, a mistake in Werkheiser's treatment of model I was spotted and corrected [4]. Unfortunately, this integration procedure is inappropriate for model IV. Because of the extreme range in maximal velocities found in model IV, the resulting differential equations are difficult to integrate numerically (a condition known in mathematical jargon as "stiffness") and require special routines. One such routine, commonly called the Gear routine, is presently being adapted by us for the intergration of model IV.

Results under steady state conditions were largely obtained with a pattern search optimization routine [17, 18]. This program, STEP 50 [3, 17], works as follows:

(1) The first call on STEP 50 initializes all internal variables and calls for the computation of the minimizing function, for the initial values or first guesses of the variables for which we are solving (the range of each variable is included as input).

(2) A set of exploratory moves is made adjusting the variables one at a time. The value of Y is computed after each move. A particular move is retained if it results in a lower value of Y than existed before the move. For equal or higher values of Y, the move is rejected.

(3) If the new value of Y is decreased, then the corresponding individual variable values replace the initial starting values to become the new base point.

(4) A pattern move is now made that adjusts the variables by the amount each has changed between the starting point of "first guess" and the first base point, or between two successive base points. The pattern move is followed by another set of exploratory moves, and the value of Y after the pattern move is used as the starting comparison for this new set of moves.

(5) The value of Y at the end of the exploratory

moves is compared with the best base point and recorded as a new base point if an improvement has been made. This is followed by another pattern move and so forth.

(6) If the above test fails, the pattern move and succeeding exploratory moves are rejected. The variables are set back to their last base points and a new set of exploratory moves are tried.

(7) If $| Y_{old} - Y_{new} | / Y_{old} < \Sigma$, an input, the search is stopped and the system considered solved.

In our case, the minimizing function Y is taken as

$$Y = \sum_{i=1}^{N+1} G_i^2,$$

where we are summing over the number of intermediates N + 1, and where $G_i = d(\text{intermediate})_i/dt$ $(i \leqslant N)$ and $G_{N+1} = v_{DNA} - V_{ss}$ (V_{ss} = constant = velocity at which the steady state condition is tested). At steady state, when all intermediate concentrations and v_{DNA} are constant, **Y** goes to 0.

The extreme versatility of this routine is recognized when we realize that we may choose any parameters as variables.

Thus, it is a simple matter to investigate steady state drug actions in the manner reported in Results. As an idea of what is involved, we describe the generation of two drug isobols at the 50 per cent inhibitory level. The procedure begins with the simulation of steady state with no drugs present. In this way, we solve for all steady state intermediate concentrations and for the velocity of DNA formation at steady state. Our next move is to fix the velocity of DNA formation at one half of its uninhibited steady state value, while assigning one of the drug concentrations as a variable. This yields the predicted 50 per cent inhibitory dose of that particular drug for DNA synthesis. Repeating this procedure with each of the other drugs gives us all 50 per cent inhibitory doses. Note that our choice of 50 per cent inhibition is completely arbitrary and we could just as easily repeat the entire procedure described above and below at any desired level of inhibition.

Now we are ready to compute the 50 per cent inhibitory level for two-drug isobols. These isobols represent the set of points, (x, y), where x and y are those concentrations of drug 1 and drug 2, whose combination will yield a 50 per cent inhibition of DNA synthesis. Then, by fixing the first drug at some concentration below 1, we solve for the necessary concentration of the second drug which will provide a steady state at conditions of 50 per cent inhibition. The shape of this isobol reflects the qualitative types of interaction, either antagonistic, synergistic or additive, between the two drugs (as discussed in Results).

Because we are dealing with highly nonlinear algebraic equations, there is no reason why our steady state solutions need be unique. The STEP 50 routine, by allowing us to begin our search anywhere within the appropriate variable range, provides an easy means of checking the multiplicity of the steady state. However, all of our models tested to date have had unique solutions. The accuracy of our solution has been confirmed by the fact that similar data has been obtained with an an alternative optimization routine based on Bremermann's global optimization method [19] and loaded into a PDP11/40.

Biochemical determination of various constants

The real numerical values of all maximal velocities, Michaelis–Menten constants, and nucleotide inhibitor and activator feedback constants have been obtained either from the literature or proper experimentation [20–26]. Table 1 summarizes the numerical values of all relevant enzyme kinetic parameters as used to obtain convergence to a steady state for model IV. It must be remembered that the activity of ribonucleotide reductase is influenced by many factors, including its instability, the dithiol (thioredoxin) concentration, Mg^{2+}, Fe^{2+} and various other ions, in addition to all the nucleotides. The measured activity also varies with tissue and tumor growth, and fluctuates during the cell cycle. Thus, the quoted values of maximum velocities can only be taken as an approximate order of magnitude, and in this range they were used.

The K_m values and the activation and inhibition constants are more reproducible [20], even with the limited data on their interactions with varied activator and inhibitor levels. The latter are the concentrations giving 50 per cent activation, or 50 per cent inhibition at optimal activator concentration, for triphosphates, ignoring any conversion to diphosphates.

The V_{max} values for Novikoff reductase have been calculated from the observed level of CDP reduction in the 100,000 *g* supernatant fraction and the ratios of CDP-UDP-ADP-GDP reduction with purified enzyme. The later ratio varies with the cell cycle phase (see Table 2). The ribonucleotide concentration for Novikoff cells was determined by R. B. Hulbert, using liquid chromatography.

RESULTS

Uninhibited steady state

As shown previously [4] all results pertaining to steady state conditions with model I were reproduced using STEP 50. For an in depth discussion of model I results, however, one should refer to Werkheiser's original paper [3].

Prelimimary studies of different versions of model II were carried out with regard to its overall "stability", as judged by the presence or absence of a steady state. These findings are presented in Table 3. Out of the possible combinations of feedback inhibition constants producing a stable model, one was selected, largely on the basis of its accord with current biochemical knowledge, as the model for which all simulations were run. Note, however, the sensitivity of the model to parameter changes, contrary to what has been reported in the literature for earlier models [3]. For instance, reducing K_{cc}, the feedback of DCTP back onto the CDP → DCTP reaction, from 1 to 0.1, maintains a convergence of the steady state, while a further reduction to 0.01 destroys the steady state (Table 3). Given this dependence, it is obvious that parameter values may be critical in determining the behaviour of a system.

During studies of model III, this dependence on parameter values was observed as well. Data obtained from different cell lines (synchronized in Mid-S phase-

Table 1. Real numerical values of enzyme kinetics parameters, as determined by direct experimentation with various cell lines (Experimental) or by indirect computation from known Experimental data (Estimated) as utilized or modified to obtain stability for model DNAMET IV.

	Maximum velocity (μM/min.)					
	Experimental	Estimated	Utilized	Cell line	Comments	Ref.
V_{max}^{DUDP}		0.93	0.93	Novikoff	Log-phase	20
V_{max}^{DUDP}	17,500		17,500	Ascites	Log-phase	22
V_{max}^{DCDP}	0.83		0.6	Hepatoma	Log-phase	20
	3.0			Chin. hmstr.	Mid-S	23
V_{max}^{DCTP}		17,500	39,000		(By analogy with dUTP formation)	22
V_{max}^{DCMP}	7,000		7,000	Chin. hmstr.	Mid-S	21
V_{max}^{DUMP1}	2,500		2,500	Chin. hmstr.	Mid-S	21
V_{max}^{DUMP2}		12,500	12,500			
V_{max}^{DTMP1}		2,500	2,500			
V_{max}^{DTMP2}		3	0.3			
V_{max}^{DTDP1}		7,000	7,000			
V_{max}^{DTDP2}		0.83	0.83			
V_{max}^{DTTP}		17,500	17,500			20
V_{max}^{DGDP}		1.63	1.63	Novikoff		20
V_{max}^{DADP}		0.6	0.6	Novikoff		
	1.26			Chin. hmstr.	Mid-S	26
V_{max}^{DATP}		17,500	12,500		(By analogy with dUTP formation)	
V_{max}^{CD}		3,000	3,000		(1,000 nucleotides/min/mole polymerases)	
V_{max}^{TD}		3,000	3,000	Mol. wt./α-polymerases = 55,000 daltons		
V_{max}^{GD}		3,000	3,000	Mol. wt./β-polymerases = 40,000 daltons		
V_{max}^{AD}		3,000	3,000			
V_{max}^{ATP}		17,500	17,500			

	Michaelis constant (μM)					
	Experimental	Estimated	Utilized	Cell line	Comments	Ref.
K_m^{UDP}	40		40	N.A.H.		20
K_m^{DUDP}		510	510	N.A.H.		22
K_m^{CDP}	10		10	N.A.H.		20
K_m^{DCMP}	400		300	Chin. hmstr.		21
K_m^{DUTP}		800	800		K_m are those from the activator	21
K_m^{DUMP}		800	800	(By analogy	level, which gave the lowest K_m	21
K_m^{TDR}		800	800	with	in their experiments	21
K_m^{DTDP}		800	800	dCMP → dCDP)		22
K_m^{TDP}		15	15			

K_m^{GDP}	30		30	N.A.H		20
K_m^{DGDP}		330	330			22
K_m^{ADP}	80		80	N.A.H.		20
K_m^{DADP}		60	60			
K_m^{DCTP}		90	90			
K_m^{DGTP}		90	90			
K_m^{DATP}		90	90			

	Feedback inhibition constants (μM) Experimental	Estimated	Utilized	Cell line	Comments	Ref.
K_{uu}	20		20	N.A.H.	Concentration giving 50%	20
K_{tu}	20		20	N.A.H.	activation, or 50% inhibition at optimal activation	20
K_{gu}	3		3	N.A.H.	concentration	20
K_{au}	20		20	N.A.H.		20
K_{tc}	50		50	N.A.H.		20
K_{gc}	5		5	N.A.H.		20
K_{ac}	10		10	N.A.H.		20
K_{td}		50	50		(By analogy with K_{tc})	
K_{tr}		20	20		(By analogy with K_{tu})	
K_{gg}	40		40	N.A.H.		20
K_{ag}	4		4	N.A.H.		20
K_{aa}	9		9	N.A.H.		20
K_{cc}	Very small inh.		10^3			

	Feedback activation constants (μM) Experimental	Estimated	Utilized	Cell line	Comments	Ref.
R_{tg}	20		20	N.A.H.	(In presence of 2 mM ATP)	20
R_{ga}	0.8		0.8	N.A.H.	(For GTP $\sim$ 0.25 mM)	20

	Ribonucleotide concn (μM) Experimental	Estimated	Utilized	Cell line	Comments	Ref.
UDP	210		590	N.A.H.		R. B. Hurlbert, private communication
CDP	80		60	N.A.H.		
TDR		4,000	4,000			
TDP		4,000	4,000			
GDP	290		80	N.A.H.		20
ADP	980			N.A.H.		20
	1,300		800	Chin. hmstr.		25

B.P. 28/19—C

Table 2. Final concentrations of the four deoxyribonucleotides pools as given by the different models (upper panel) and as experimentally found in different cell lines (lower panel)*

	DATP	DGTP	DTTP	DCTP	V_{ss}
Model I	0.4214	None	0.4214	0.9375	0.3404
Model II	1.713	0.106353	0.4682	0.7387	0.3189
Model III	0.002	0.60206	1.0838	0.8169	0.4458
Model IV	$\leqslant 0.514 \times 10^{-3}$ (mM)	0.1203×10^{-4} (mM)	0.4173×10^{-5} (mM)	0.6072×10^{-5} (mM)	0.2726×10^{-3} (mM/min)

	DATP	DGTP	DTTP	DCTP
HeLa [27]	$4.2 10^{-3}$ mM (0.724)	$4.2 10^{-3}$ mM (0.724)	$8.4 10^{-3}$ mM (1.45)	$5.8 10^{-3}$ mM (1.0)
CHO [28]	$9.1 10^{-3}$ mM (0.23)	$1.3 10^{-3}$ mM (0.03)	$4.2 10^{-3}$ mM (0.10)	$42 10^{-3}$ mM (1.0)
Mouse embryo [29]	$4.1 10^{-3}$ mM (0.352)	$0.63 10^{-3}$ mM (0.053)	$3.5 10^{-3}$ mM (0.29)	$11.7 10^{-3}$ mM (1.0)

* Note that the final concentrations given by model IV (last row upper panel) are *not* in arbitrary units. The value of steady state velocity (0.27) mM/min) corresponds to a diploid cell line which last 8 hr in S-phase (during which 151 mM of new DNA is replicated, and will synthesize DNA at a velocity of 0.32 mM/min. The values in parentheses refer to the ratio of experimental nucleotide pool as referred to DCTP as units.

see Table 2) indicates a large variability which may be properly simulated only by more comprehensive and flexible models including real numerical values (which will differ between cell lines).

This brings us naturally to a discussion of model IV. Here, as described before, we are dealing with an *in vivo* simulation using real constants which may differ from each other by as much as five orders of magnitude. Given the nonlinear nature of the system and the large range of constants, a complexity and stiffness are introduced into the model far exceeding that of any of the earlier models. Despite the difficulties this presents, we have been encouraged by our results to date.

Using values close to the unaltered experimental values (see Table 1) for our constants, we have achieved a steady state (Y minimization function $= 10^{-21}$). In the instances in which we did have to use a different constant value than the experimental in order to achieve a steady state, we still maintained the value of the constant within the experimental range suggested. Specifically, the Michaelis and feedback constants were fixed exactly equal to the experimental values suggested, and the maximal velocities varied within one order of magnitude.

One problem encountered was the questionable existence of a feedback from DCTP back onto the CDP → DCDP step. The literature is vague on this point, generally speaking of a very small feedback, if

Table 3. Effects of changes in the feedback pathways on the overall convergence of model II to a steady state.*

R_{ga}	R_{gt}	K_{aa}	K_{ag}	K_{gg}	K_{ua}	K_{cc}	K_{gu}	K_{au}	K_{uu}	K_{tu}	K_{tc}	K_{gc}	K_{ac}	Computer optimization
1	1	1	1	1	0	0	1	0	1	1	1	0	1	Unstable
1	1	1	1	1	0	1	1	1	1	1	1	1	1	Unstable
1	1	1	1	1	0	1	1	1	1	1	1	1	0	Unstable
1	1	1	1	1	0	0	1	1	1	1	1	1	1	Unstable
1	1	1	1	1	0	1	1	1	1	1	1	0	0	Unstable
1	1	1	0	1	1	0	0	0	1	1	1	0	0	Unstable
1	1	1	0	1	0	0	0	0	1	1	1	0	0	Unstable
1	1	1	1	1	0	0	1	0	1	1	0	1	1	Unstable
1	1	1	1	1	0	0	1	0	1	1	1	1	0	Unstable
1	1	1	1	1	1	1	1	1	1	1	1	1	1	Unstable
0	0	1	0	1	1	1	0	0	1	1	0	0	0	Stable
1	1	1	0	1	0	1	0	0	1	1	1	0	0	Stable
1	1	1	0	1	1	1	0	0	1	1	1	0	0	Stable
1	1	1	1	1	0	1	0	0	1	1	1	0	0	Stable
1	1	1	1	1	0	1	1	0	1	1	1	0	0	Stable†
1	1	1	1	1	0	0.1	1	0	1	1	1	0	0	Stable
1	1	1	1	1	0	0.01	1	0	1	1	1	0	0	Unstable

* The investigation of the stability properties was performed by linearization of the differential equations around the steady state values and using the criterion that the eigenvalues of the Jacobian matrix associated with the system should all have negative real parts to guarantee stability [24]. Note that in the last three rows the changes affect *only* the magnitude of the feedback constants.

† Combination utilized to generate isobols.

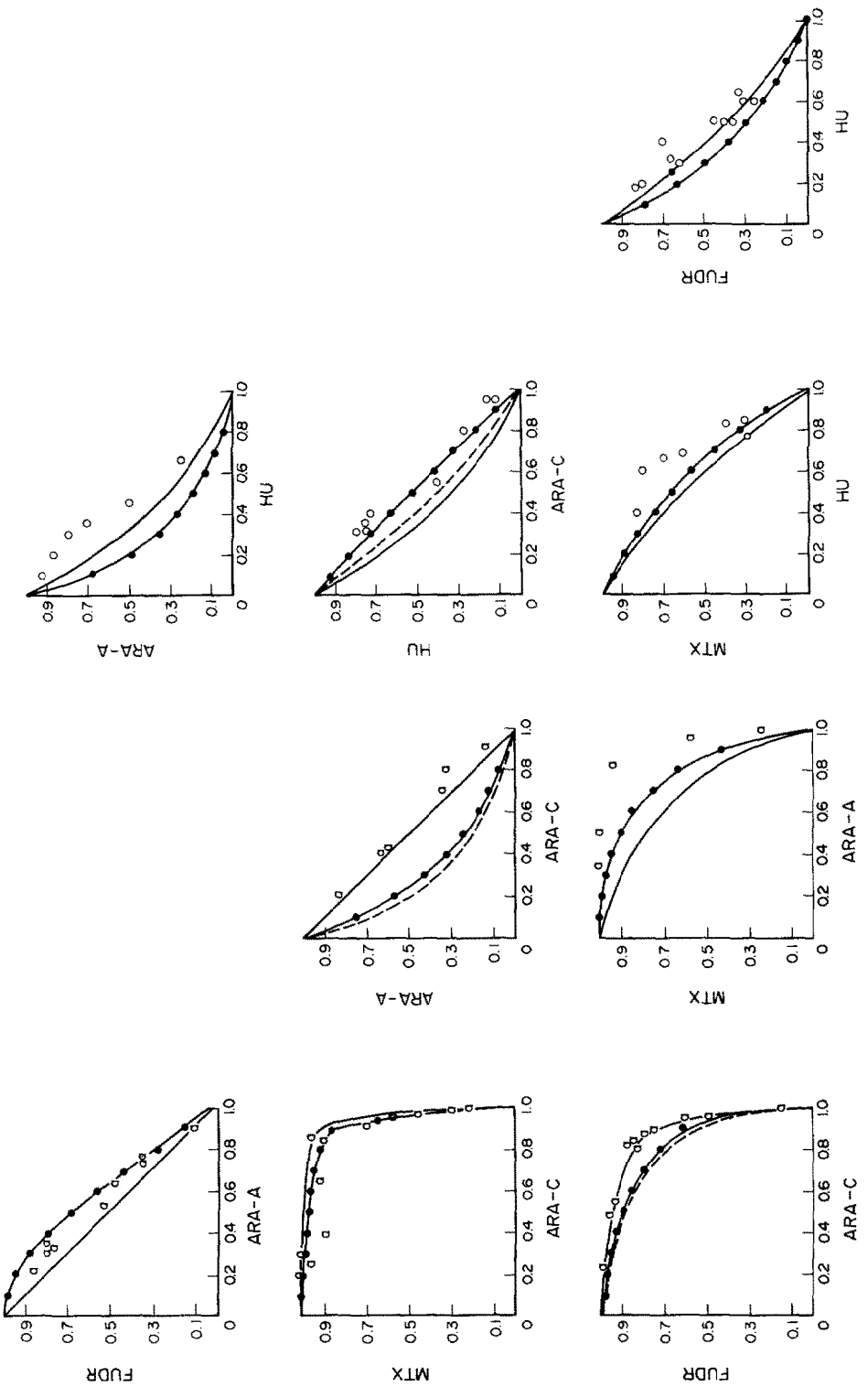

Fig. 3. Two-drug isobols generated by model DNAMET I (——), model DNAMET II with ARA-C competitive on ligase (- - -) and not competitive (·—·), compared with the *in vitro* experimental results (○). Coordinates are fractions of the 50 per cent inhibitory dose.

any. As in all of our other models, however, we found that this feedback contributes a considerable stability to the system and, therefore, we included it in model IV. We were able, though, to reduce the magnitude of this feedback to several orders of magnitude smaller than any other in the model and to well below the detectable limit of current experimental procedures.

The final steady state concentrations of the triphosphate pools, expressed in mM, and the final steady state velocity of DNA synthesis expressed in mM/min (arrived at through this model) confirmed the overall validity of the model (see Table 2): for instance, the theoretical DNA synthetic rate (0.27 μM/Min) is compatible with that one experimentally determined for a diploid cell line (0.32 μM/min) with an 8 h long S-phase. The imbalance in pool sizes, with respect to experimental values, is not totally unexpected in light of the lack of accuracy of much of the experimental data from which the constants are drawn and, perhaps more important, the fact that the constants are compiled from data collected from several different cell lines (principally Novikoff and Chinese hamster). This last point is critical, as we find that slight variations in constant values, particularly in the initial steps of the network, may lead to drastic changes in the steady state intermediate concentrations without affecting the convergence of the system to a steady state. Hopefully, we will soon have consistent experimental data, collected from a single cell line, on which to base our model. We would like to reemphasize, though, that this variability suggests that the quantitative or even qualitative behaviour of the system may depend on quantitative differences in constant values and that drug action, therefore, may differ between cell types.

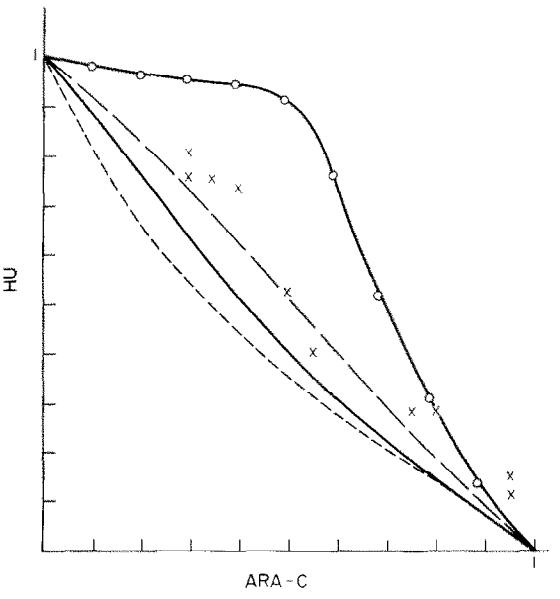

Fig. 4. Two-drug isobol generated by model DNAMET II utilizing real valued constants. More details are given in the text. Key: (ø——ø) Model II with real valued constants; (— —) Model II with constants set = 1; (——) Model II with constants set = 1, ARA-C competitive on ligase; (- - - -) Model I (Werkheiser's model); and (×) experimental values.

Two-drug isobols

Several two-drug isobols from model II are plotted in Fig. 3 along with the isobols calculated by model I and with model II where ARA-C is taken as acting competitively on ligase. Included also are the actual experimental isobols for suspension cultures of leukemia L1210 cells [5]. It was to explain these experimental results, which in certain cases were opposite to those predicted by traditional arguments of sequential, concurrent and complementary inhibition, that Werkheiser designed model I [3].

From these studies we see what effect slight changes in the model may have on a two-drug isobol structure. The changes we are referring to here are small structural alterations in the model, such as between model I or model II with ARA-C acting competitively or noncompetitively on the ligase reaction. Judging from the effects of quantitative differences on stability of the models, as discussed in the previous section, one might expect an influence on isobol form due to quantitative differences. In fact, this premise is borne out by the ARA-C vs HU isobol generated from the adaptation of model II using real constants (shown in Fig. 4). Note that this isobol is the only isobol predicting antagonistic behaviour for the entire range of ARA-C values and that it is qualitatively different from the isobol generated by the same model with arbitrary values.

Such results, indicating that small model changes may lead to differences in isobols as well as differences in its convergence to a steady state, as discussed previously, force one to question whether it is valid to design the mathematical model primarily through an optimization of its predictions with steady state isobol experimental data, an approach chosen by the Werkheiser group. (Indeed, their claim that their models are relatively insensitive to parameter changes is questionable, in light of this approach.) A strategy of this nature gives no guarantee that the model arrived at will yield accurate simulation of transient situations nor does it guarantee that it will provide valuable guidelines toward designing a working *in vivo* model. Rather, a logical approach must include constant feedback between the structure of the real biochemical system, as presently understood, and the emerging theoretical model. Inclusion of all proper metabolic pathways and feedback is necessary in order to mimic the actual interactions occurring within the cell.

At this point it is convenient to introduce two notes of caution which will have to be kept in mind for future studies. First, in regard to future results from models III and IV, it will not be proper to compare *in vitro* experimental results with predictions from a theoretical model aimed toward simulating *in vivo* conditions. With regard to this difficulty, we expect soon to have experimental results under *in vivo* conditions by means of special techniques already outlined in the literature [4]. This will be of great benefit in helping us to discriminate between different *in vivo* models.

The second difficulty has to do with the way the original experiment was carried out [5]. It appears from the original paper that what was measured was 50 per cent inhibition of cell growth rather than 50 per cent inhibition of DNA synthesis. By not accounting for the fraction of time the cell is in S phase, what the authors

actually measured were the isobols at a higher level of inhibition. Using data taken from Ref. 30, which reports S phase as roughly 9 hr and the total cycle time as 12 hr, we can compute the actual level of DNA inhibition for the above experiment as being about 57 per cent of DNA synthesis inhibition, rather than the 50 per cent reported.

If the theoretical isobols remained unchanged with increasing levels of inhibition, this difference would be irrelevant. However, as first pointed out by Werkheiser *et al.* [3] and verified by us also with model II, a different per cent of inhibition may lead to quantitative (although probably not qualitative) differences in the isobols. Thus, an interaction such as FUDR vs HU showed a greater degree of synergism at 80 per cent than at 50 per cent. Of course, such findings are directly relevant to the problem of establishing clinical drug protocols.

Three-drug interactions

In our use of isobols to study drug interaction, we are by no means limited to two-drug interactions. In theory, the same general principles may be applied to interactions involving an arbitrary number of drugs. We now address ourselves to the problem of a three-drug isobol, i.e. a surface in three dimensions which is a level set in regard to degree of DNA synthesis inhibition (V_{ss} = constant = f(D1, D2, D3)). The method used to produce these surfaces is merely an extension of the procedure for the calculation of two-drug isobols discussed earlier.

Suppose we are interested in a three-dimensional isobol at the 50 per cent inhibitory level of the three drugs, where $X^1_{50\%}, X^2_{50\%}, X^3_{50\%}$ denote the appropriate inhibitory dosages for the three drugs. We can plot the three-dimensional isobol simply by setting $X^3 = (X^3_{50\%})\,K$, $K = 0, 0.1, \ldots, 0.9$, and then solving the equations for the two dimensional isobols for X^1 and X^2. We thereby obtain the contour plot of the three-dimensional isobol in the X^1, X^2 plane with X^3 at various levels between 0 and $X^3_{50\%}$. In order to more readily study these three-dimensional isobols, we found it convenient to introduce a quantitative index of drug action. However, before describing our choice of index, we first must declare the particular definitions of synergism, antagonism and additivity that we have adopted. N drugs are considered to be acting additively in a given region if their isobol at the desired level of inhibition can be described in this region by the hypersurface, $A_1 + A_2 + \ldots + A_n = 1$, where all A_i values represent normalized drug doses. Moreover, N drugs are considered to be acting synergistically in a given region if the isobol satisfies the condition $A_1 + A_2 + \ldots + A_n < 1$ at any point on its surface, and antagonistically if for pts. on its surface $A_1 + A_2 + \ldots + A_n > 1$.

As an example, in two dimensions, an isobol lying below the line, $A_1 + A_2 = 1$, would be considered synergistic, while an isobol above the line, $A_1 + A_2 = 1$, would be antagonistic. It is important to note that it is not necessarily the curvature of the isobol which determines the manner of drug interaction, but rather its location in the drug phase space relative to the additive isobol.

Using the above definitions, we can establish an overall drug index which will relate the departure of a given isobol from the strictly additive isobol to its degree of synergism or antagonism. We do this by first defining at any given point lying on the isobol surface, a subindex, l_i given by:

$$l_i = (A_1 + A_2 + \ldots + A_n) - 1$$

Then an overall approximate drug index, L, can be defined by an average of subindex values for M points evenly distributed about the entire isobol. That is,

$$L = \sum_{J=1}^{M} lj/M$$

(To make this exact we could use the integral in place of the finite sum.)

By this definition, synergistic combinations of drugs would have indexes ranging from -1 to 0, an additive combination an index of 0, and antagonistic combinations, indexes greater than 0.

Of course, since we are using an average, we must be aware of the possibility of synergistic and antagonistic regions cancelling each other. Thus, an interaction of two drugs might have a total index close to 0, although in certain regions the drug combination was either strongly synergistic or antagonistic.

This problem can easily be taken into consideration by dividing an isobol into regions where one or the other of the types of drug interactions dominates, and considering each of these regions seperately.

An advantage of the method described above for characterizing drug interactions is that it can easily be applied to describe the interactions of an arbitrary number of different drugs.

In fact, for a drug dimension greater than 2, we can use the above general method for more than one kind of labeling index (N-1 kinds, to be exact). For instance, in three dimensions we can either define an index which will indicate the overall interaction of the three drugs ($L = \Sigma l_i$: where $l_i = A_1 + A_2 + A_3 - 1.0$) or alternatively by defining, $L(A_3) = [\Sigma l_i(A_3)]$ (where $l_i = A'_1 + A'_2 - 1.0$, and A_3 is held constant over the sum), we can consider the influence of a third drug on the type of interaction of two other drugs. Note that for this last type of index, we are renormalizing A_1 and A_2 for each value of A_3.

As an example of the ideas outlined above, we can consider the 50 per cent three-dimensional isobols generated by model DNAMET II for the drugs ARA-A, ARA-C, FUDR and HU.

Examining the graphs below (Fig. 5), we see that the third drug under consideration is critical in determining both the strength and type of interaction of two other drugs. These graphs consist of plots of the value of the two-dimensional index, $L(A_3)$, defined above, vs concentrations of the third drug.

In all cases except for the ARA-A vs FUDR interaction, $L(A_3)$ changed significantly with changing doses of the third drug. With certain drug concentrations these changes were qualitatively similar for both of the two possible third-drug combinations. For instance, the ARA-A vs ARA-C combination showed a decrease in its synergism with increasing concentrations of either HU or FUDR, as did the combination HU vs ARA-A with increasing concentrations of ARA-C or FUDR. Similarly, the combination of FUDR vs ARA-C

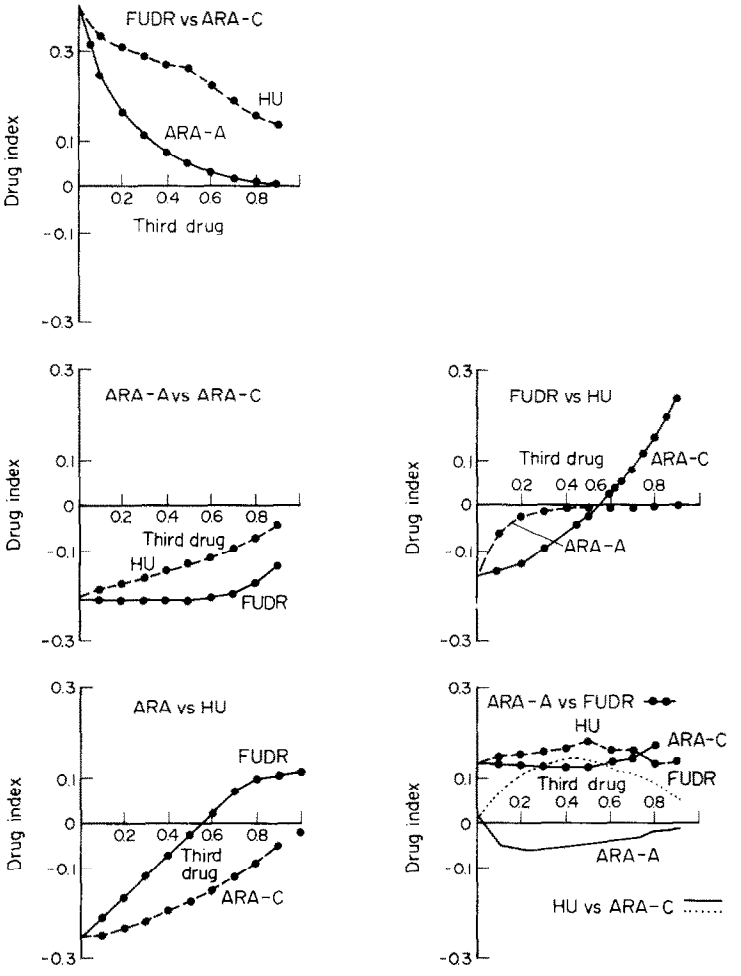

Fig. 5. Three dimensional isobols generated by model DNAMET II. The symbols near each curve refer to the third drug considered; the scale on the X-axis gives its value as a fraction of its 50 per cent inhibition value.

showed a decrease in antagonism with increasing concentrations of HU or ARA-A.

However, quantitatively these changes were markedly different for the two possible third-drug combinations. For the ARA-A vs ARA-C interaction, FUDR produced a much greater drop in synergism with increasing concentrations than did HU.

Likewise, the drop in antagonism with increasing concentrations of the third drug for the interaction of FUDR vs ARA-C was much stronger with ARA-A as the third drug than with HU. Indeed, the interaction became nearly additive at high doses of ARA-A, while still remaining strongly antagonistic with HU. The most dramatic differences in the quantitative degree of these changes, however, was shown in the HU vs ARA-A interaction. Here, FUDR as the third drug produced such a sharp decrease in synergism that at very high concentrations the interaction actually became antagonistic. In contrast, ARA-C as the third drug caused a much slower drop in synergism and the interaction remained significantly synergistic even at a ARA-C concentration of 0.9.

In two cases, the changes in the type of interaction were actually qualitatively different for different third drugs. For the FUDR vs HU interaction, ARA-A produced a shift from synergism to additivity, while ARA-C produced a shift from synergism to strong antagonism. Most intriguing though was the effect of third drugs on the HU vs ARA-C interaction. This interaction with no third drug present was very nearly additive. With ARA-A as the third drug, this interaction became strongly antagonistic while with FUDR it was synergistic. Thus, two different choices of the third drug precipitated entirely opposite changes in the two-drug interaction.

Such studies indicate that pertubations of the system may be used to alter drug action. In this case, the perturbation is created by the presence of the third drug. However, these studies suggest as well that time sequence drug administration, where the first drug is used to perturb intermediate pool sizes, may also be an effective means of altering drug action. This point will be elaborated upon in a later section.

An analysis of the overall drug index for the various three-drug combinations is also interesting. Such an analysis reveals that the overall interaction, whether it is synergistic or antagonistic, is strongly dependent on the exact concentration of the three drugs and not only

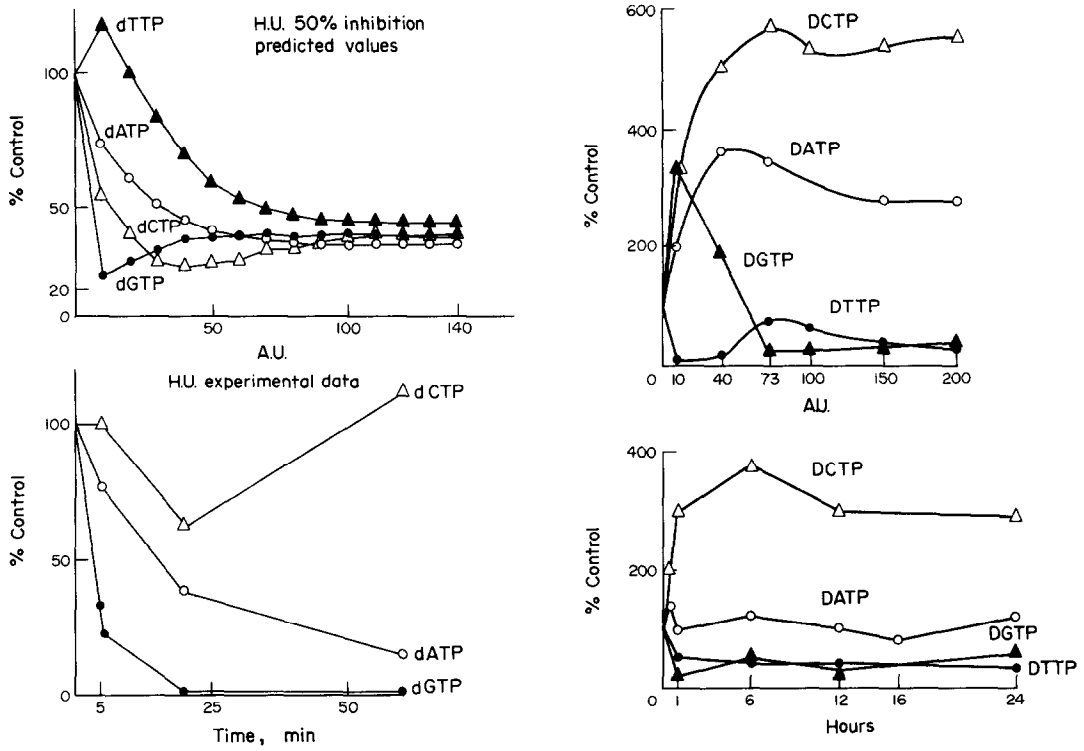

Fig. 6. Comparison between the time evolution of the four deoxyribonucleotides as predicted by model II (upper panels), and the experimental results (lower panels) following administration of hydroxyurea (left panel) and methotrexate (right panel). A. U. = arbitrary units.

on their sites of action. This fact, therefore, should be considered when utilizing multiple drug combinations in anti-neoplastic treatment. Although in all cases the greatest degree of either synergism or antagonism occurs for two-drug combinations, this does not foreclose the importance of three-drug combinations in achieving maximum synergism in other, perhaps more realistic models. Therefore, this is also an avenue which should be explored further.

Nucleotide pools vs time after perturbation

As stated previously [3], investigations of time sequence behaviour of intermediates involved in DNA synthesis are extremely important. Due, no doubt, to the extensive feedback found in DNA synthesis, concentrations may oscillate or overshoot before reaching steady state values. Thus, experiments which predict drug effect by the direction of initial changes in pool sizes may be highly misleading [3]. This is illustrated by Fig. 6 where a comparison is shown between the time evolution of the four deoxyribonucleotide pools after inhibition by MTX, as predicted by model II and as experimentally determined for mouse 5178Y lymphoma cells [31]. Of course, this is at best an indirect comparison, as the drug concentration used in the experiment was not the 50 per cent inhibitory dose for MTX. However, the model seems to be able to mimic, at least qualitatively, the experimental data. A comparison with the time course predicted for the dCTP, dGTP, dATP and dTTP pools by model I [3, 4] strongly suggests a greater capability of model II in describing the processes involved in the DNA inhibition by the drug.

More precisely, the final portion of the overshoot of the dCTP pool after about 12 hr and the intersection of the dGTP and dTTP curves after about 16 hr seem to be predicted by the model. Also, in the case of 50 per cent inhibition by hydroxyurea, the time sequence of the same nucleotides, as simulated by DNAMET II, is in approximate agreement with the experimental data obtained [29] (see Fig. 6). These two examples indicate the overall capability of simulation, even at the simplest level, to predict the experimental variations of intermediates as a consequence of drug perturbation. Indeed, the nucleotide pools reach the new steady state in a quite shorter time scale after hydroxyurea administration than after methotrexate administration (see also below), both in the experimental evolution (lower panels) and theoretical simulation (upper panels).

Interaction of drugs given sequentially

In terms of potential therapeutic action, time sequence drug administration may be of extreme value. Our theoretical models suggest that pertubation of intermediate pool sizes by one drug will affect transient behaviour after administration of a second drug. This will be especially significant if the time to reach steady state is large relative to the duration of S phase (which below), both in the experimental evolution (lower panel) and theoretical simulation (upper panels).

Table 4. Effects of the order of sequence of two drugs (HU and ARA-C) on the rate of DNA synthesis*

State of the system	%DNA synthetized after 20 A.U.	% DNA synthetized after 40 A.U.	State of the system	% DNA synthetized after 38 A.U.	% DNA synthetized after 76 A.U.
No drugs	100	100	No drugs	100	100
HU ($t = 0 \rightarrow t = 20$)			HU ($t = 0 \rightarrow t = 38$)		
ARA-C ($t = 21 \rightarrow t = 40$)	50	46	ARA-C ($t = 39 \rightarrow t = 76$	50	48
ARA-C ($t = 0 \rightarrow t = 20$)			ARA-C ($t = 0 \rightarrow t = 38$)		
HU ($t = 21 \rightarrow t = 40$)	44	54	HU ($t = 39 \rightarrow t = 76$)	47	45
50% HU + 50% ARA-C			50% HU + 50% ARA-C		
($t = 0 \rightarrow t = 40$)	50	51	($t = 0 \rightarrow t = 76$)	51	51

State of the system	% DNA synthetized after 270 min	% DNA synthetized after 540 min
No drugs	100	100
HU ($t = 0 \rightarrow t = 270$)		
ARA-C ($t = 271 \rightarrow t = 540$)	50	36
ARA-C ($t = 0 \rightarrow t = 270$)		
HU ($t = 271 \rightarrow t = 540$)	34	22

* The upper panels refer to a simulation utilizing model DNAMET II with all the constants set equal to 1. The lower panel refers to an analogous simulation utilizing a real-values model, as explained in the text. The values of the drugs are those which gave a 50 per cent inhibition steady state.

per cent inhibition at steady state may give rise to extremely different percentages of DNA synthesis over a biologically significant time scale.

To study sequential drug administration we are first framing the problem as follows: given a pulse of drug 1 at $t = 0$, at what time, t, would administration of a second pulse of drug 2 yield the minimum DNA synthesized during a given time interval, ΔT? (Alternatively, we might fix the total amount of DNA synthesized, and maximize the time interval required for synthesis.)

At first, h_1, t_1 and h_2, t_2, where h_i is the concentration and t_i is the time interval for administration of the ith drug, would be fixed and the optimum time t found. This could eventually be extended by allowing h_1 and t_1, and h_2 and t_2 to vary, subject perhaps to the constraints $h_1 t_1 = D_1 =$ constant, and $h_2 t_2 = D_2 =$ a constant. Finally, instead of using square pulses, more realistic pulse shapes predicted by drug metabolic experiments could be used. Ultimately, such studies may be able to provide the optimum chemotherapy strategy, predicting not only which drugs to choose, but also the time and manner for the administration of each of these drugs.

Early studies have been carried out with model II, using the drugs HU and ARA-C. Whereas HU causes generally a monotonic shift to the new 50 per cent inhibited steady state, ARA-C achieves a new steady state only after oscillations of pool sizes (not shown). Moreover, the time scale necessary for this shift is greater for ARA-C than HU, as shown by utilization of real numerical values (see below). Initially, by comparing our simulation of MTX inhibition with experimental results, we obtained a rough correspondence between the arbitrary units (A.U.) of model II and real time, establishing 100 A.U. equivalent to 12 hr.

Choosing the time for integration first equal to 9 hr (duration of typical S-phase), we then proceeded in our simulation, as outlined above. Starting from the uninhibited steady state, we first applied a 50 per cent inhibitory dosage of HU from $t = 0$ to 38 A.U., followed by an equivalent dosage of ARA-C from $T = 38$ to 76 A.U. This was repeated with the two drugs interchanged and both cases were then compared to simultaneous administration of one-half the 50 per cent dosages of both HU and ARA-C from $T = 0$-76 A.U. Note that, at these dosages, the two drugs are nearly additive at steady state.

The results are shown in Table 4. We see that there are small but significant differences between the two sequences of HU and ARA-C. This is not surprising given the relatively long time necessary for ARA-C to cause a shift to a new, inhibited steady state. What is surprising is that the ARA-C-HU sequence results indicate that the time scale for going to the inhibited steady state becomes large for HU if one begins with intermediate pool sizes determined by the ARA-C perturbation rather than the uninhibited steady state pool sizes.

We then repeated this simulation with the total time interval for integration reduced to 40 A.U. The results are also shown in Table 4. What is now interesting is

that, while the effectiveness of the HU–ARA-C sequence is qualitatively independent of the time interval chosen, the ARA-C–HU sequence effectiveness is strongly dependent. For a short time interval the administration of HU after ARA-C is much less effective than for a long time interval, while for the reversed sequence the short and long time intervals yield similar results, both giving a greater inhibition than simultaneous administration of both drugs.

Encouraged by these findings, we then repeated the above study over a 9-hr time interval, using a version of model II with real constants, described earlier in this paper. In this case, where the time scales for transient behaviour of the system (starting from unperturbed steady state values) after administration of HU and ARA-C are drastically different (HU few minutes, ARA-C many hours), the results are far more dramatic, and a critical dependence on drug ordering is now demonstrated (Table 4). The dependence is similar to that predicted from the earlier study for a long time interval.

Given that these results were obtained using an early model, we must emphasize that our point was not to obtain definite predictions of the interactions of specific drugs administered sequentially. Rather we desired to demonstrate that, given two drugs with different transient behaviours, their interaction may be strongly sequence dependent, mainly when real numerical values are utilized, and that possibly this feature may be taken advantage of in optimizing drug action.

DISCUSSION AND CONCLUSION

In summary, our pharmaco-enzyme models demonstrate the potential for simulation of DNA anti-metabolite drug action on intermediate pool sizes and DNA synthesis.

In addition to providing a framework for the understanding of experimentally observed two-drug interactions as discussed in earlier papers [3, 4], they also allow us to make definite predictions concerning more complex aspects of drug interactions. Studies of steady state three-drug interactions, aided by our definition of a quantitative drug index, indicate that it may be possible to dramatically reverse the type as well as intensity of interaction between two drugs by increasing the concentration of a third drug. This may be understood as the effect of pertubations in intermediate pool sizes, in this case produced by the third drug, on drug interaction.

Similarly, transient deviations from steady state pool sizes may have profound influences on drug action, producing drug interactions which cannot be extrapolated from steady state results. Thus, time sequenced drug administration was shown to have great influence on drug interaction if the time scale of the system for transient behaviour was large, relative to the appropriate biological time interval. This raises the question of whether steady state results are at all meaningful biologically as it has not yet been established, experimentally or theoretically, how appropriate the steady state approximation is over the relevant time interval. Therefore, theoretical models must have as their aim the accurate simulation of transient as well as steady state conditions.

This calls for a model utilizing "realistic constants" in order to present results according to a real time scale. In light of the sensitivity of these models to small qualitative and quantitative changes in structure, as shown by convergence, two-drug isobols, and time evolution studies, it is essential for all purposes that the mathematical model be patterned as closely as possible to the real biochemical system, including all known pathways and the use of experimentally derived constant values.

This has been done with model IV which also includes the salvage pathways critical for the simulation of *in vivo* conditions. It is significant that early attempts using one incorrect feedback constant (K_{rc}) required extensive changes in other constant values before convergence to a steady state could be achieved, while substitution of the correct value led to convergence with only minor changes of the constant values. This is consistent with results obtained from models II and III concerning the sensitivity of the models to parameter changes.

Finally, we would like to reemphasize that such dependence of the system, although introducing an added complexity, suggests the possibility that differences in constant values between cell lines may lead to qualitative, in addition to quantitative, differences in drug action and interaction. However, it is only through an approach involving constant feedback between experimental results and theoretical models that such a possibility may be best explored, to enhance the effectiveness of combination cancer chemotherapy.

REFERENCES

1. S. C. Sung, *Life Sci.* **15**, 359 (1974).
2. K. R. Harrap and R. C. Jackson, *Adv. Enzyme Regulat.* **13**, 77 (1975).
3. W. Werkheiser, G. Grindey and R. Moran, *Molec. Pharmac.* **9**, 320 (1973).
4. C. Nicolini, E. Milgram, F. Kendall, W. Giaretti, in *Growth Kinetics and Biochemical Regulation of Normal and Malignant Cells* (Eds. B. Drewinko and R. Humphrey), p. 411. Williams & Wilkins, Baltimore (1977).
5. G. B. Grindey and C. A. Nichol, *Cancer Res.* **32**, 527 (1972).
6. G. Grindey, R. Moran and W. Werkheiser, in *Advance in Drug Design* (Ed. E. J. Ariens), Vol. 5, pp. 170–249. Academic Press, New York (1975).
7. O. H. Strauss and A. Goldstein, *J. gen. Physiol.* **26**, 559 (1943).
8. C. Nicolini, *Biochim biophys. Acta* **458**, 243 (1976).
9. J. J. Furth and S. S. Cohen, *Cancer Res.* **28**, 2061 (1968).
10. S. S. Cohen, *Molec. Biol.* **5**, 1 (1966).
11. R. Momparler *Cancer Res.* **34**, 1775 (1974).
12. R. L. P. Adams and J. C. Lindsay, *J. biol. Chem.* **242**, 1314 (1967).
13. W. C. Mohler, *Cancer Chemother. Rep.* **34**, 1 (1964).
14. J. W. Yarbro, *Cancer Res.* **28**, 1082 (1968).
15. C. Heidelberger and K. U. Hartmann, *Fedn Proc.* **20**, 167 (1961).
16. R. W. Hamming, *Numerical Methods for Scientists and Engineers*, 2nd Edn, p. 136. McGraw-Hill, New York (1973).
17. C. F. Wood, *Res. Memo.*, Comp. 765, Westinghouse Research Laboratory, Pittsburgh, PA (1967).
18. E. Milgram and C. Nicolini, *Internal Report 4175*, pp. 1–54. Biophysics Division, Temple University, Philadelphia PA (1975).

19. C. T. Wu, F. Kendall, W. Linden, S. Toton, S. Zietz, *Pulse Cytophotometry* **3**, 51 (1977).
20. C. Moore and R. B. Hurlbert, *J. biol. Chem.* **241**, 4802 (1966).
21. S. A. Murphree, *Ph.D. Dissertation*, University, of Texas, Houston, TX (1972).
22. M. L. Simons, *Master's Thesis*, University of Texas, Houston, TX (1972).
23. S. Murphree, E. Stubblefield and E. C. Moore, *Expl Cell Res.* **58**, 118 (1969).
24. R. Bellman, *Stability Theory of Differential Equations*, p. 79. Dover Publications, New York (1953).
25. S. A. Murphree, E. C. Moore and D. M. Peterson, *Expl Cell Res.* **83**, 186 (1974).
26. D. M. Peterson and E. C. Moore, *Biochim. biophys. Acta* **432**, 80 (1976).
27. G. Bray and T. P. Brent, *Biochim. biophys. Acta* **269**, 184 (1972).
28. K. L. Skoog, B. A. Nordenskjold and K. G. Bjursell, *Eur. J. Biochem.* **33**, 428 (1973).
29. K. L. Skoog and B. A. Nordenskjold, *Eur. J. Biochem.* **19**, 81 (1971).
30. P. Altman and D. Katz, *Cell Biol.* **16**, 1 (1976).
31. M. Tattersall and K. R. Harrap, *Cancer Res.* **33**, 3086 (1973).